



STUDY OF NEAR-FAULT EFFECT ON SLOSHING MODE OF STORAGE LIQUID IN TANKS

Juin-Fu Chai⁽¹⁾, Fan-Ru Lin⁽²⁾, Liang Shen⁽³⁾, Wei-Hung Hsu⁽⁴⁾, Zhi-Yu Lai⁽⁵⁾, Tzu-Chieh Chien⁽⁶⁾
and Zhen-Yu Lin⁽⁷⁾

⁽¹⁾ *Research Fellow and Deputy Director, National Center for Research on Earthquake Engineering (NCREE), Taipei, Taiwan, chai@ncree.narl.org.tw*

⁽²⁾ *Associate Researcher, NCREE, Taipei, Taiwan, frlin@ncree.narl.org.tw*

⁽³⁾ *Graduate Student, NTUST, Taipei, Taiwan, M10705328@mail.ntust.edu.tw*

⁽⁴⁾ *Assistant Researcher, NCREE, Taipei, Taiwan, mikehsu@ncree.narl.org.tw*

⁽⁵⁾ *Research Assistant, NCREE, Taipei, Taiwan, zylai@ncree.narl.org.tw*

⁽⁶⁾ *Research Assistant, NCREE, Taipei, Taiwan, tcchien@ncree.narl.org.tw*

⁽⁷⁾ *Research Assistant, NCREE, Taipei, Taiwan, zylin@ncree.narl.org.tw*

Abstract

The long period velocity pulse is recognized as one of the characteristics of near-fault ground motions, and hence the response of vibration modes with lower frequencies will be amplified owing to the resonant effect. In general, the sloshing frequency of storage liquid in tanks is low and the period is similar to the pulse period of near-fault ground motions. Compared to the far-field ground motions, the induced slosh height will be amplified significantly by the near-fault ground motions due to the resonant effect. Therefore, it is worth paying attention to the near-fault effect on the sloshing mode of storage liquid in tanks.

Based on the long-stroke and high-speed shaking table at NCREE, an experiment was implemented to study the resonant response of sloshing mode. The purpose of this study is to estimate the slosh height and the associated total volume of water splashing out of the tank under near-fault ground motions, and also to determine the relationship between the resonant response and the input velocity pulse.

This paper aims to describe the test setup, the selection and processing of input motions including the original near-fault ground motions, extracted velocity pulse or extracted band-pass signals for resonance analysis as well as the impulse motion for free vibration. In addition, the experimental results are compared with the code-specified values that is determined by the industrial standards and guidelines for general seismic conditions. It is expected that based on the test results, a more proper predict equation can be proposed for the seismic design and evaluation of spent fuel pool in nuclear power plants.

Keywords: sloshing mode; near-fault ground motions; spent fuel pool



1. Introduction

Fluid-structure interaction is mainly considered in seismic evaluation of a large-scale fluid-storage tank. In past earthquake experiences, damages of storage tanks or loss of liquid content were observed due to unexpected extreme fluid-structure interaction. In industrial factories, some damages at tank rooves or at the top parts of tank walls were caused by fluid sloshing [1]. During the 2007 Niigata-Chuetsu Oki Earthquake, water in the spent fuel pool on the fourth floor of the Kashiwazaki-Kariwa Nuclear Power Plant splashed out of the pool wall and caused the release of radioactive material [2].

According to the Haroun-Housner model [3], fluid-structure response of a flexible tank during seismic excitation consists of three principal modes: the sloshing mode (also called convective mode), the impulsive mode (refers to as flexible mode), and the rigid mode. The sloshing mode shape is that each side of water surface vertically oscillate in turn with a relatively low frequency. The impulsive mode shape represents a simultaneous motion of fluid and surrounding tank wall with a higher frequency depending on the flexibility of the tank wall. The rigid mode represents that the bottom water moves rigidly with the tank base under horizontal input motion. In order to assessment seismic demand caused by sloshing modes, the industrial standard, ACI 350.3-06 [4] and SPID [5], gives equations to evaluate the fundamental sloshing frequency of stored water in a rectangular tank as below:

$$f_c = \frac{\omega_c}{2\pi} = \left(\frac{\lambda}{2\pi}\right) \frac{1}{\sqrt{L}} \quad (1)$$

$$\lambda = \sqrt{3.16g \tanh \left[3.16 \left(\frac{H_L}{L} \right) \right]} \quad (2)$$

where f_c is the natural frequency of the first mode of sloshing, L is the length of a rectangular tank in the direction of motion, g is the gravitational acceleration, and H_L is design depth of stored water. Considering slosh height is most contributed by the convective parts, a simplified computation of the maximum sloshing amplitude h_{max} can be obtained by separating the impulsive and convective parts and considering the latter only [6]:

$$|h_{max}| = \frac{8a}{\pi^2 g} \sum_{n=1}^{\infty} \frac{S_{an}}{(2n-1)^2} \quad (3)$$

where a is half-width of the tank base and S_{an} is the spectral acceleration corresponding to the n^{th} liquid frequency. By ignoring higher modes, the guidelines, ACI 350.3-06 [4] and SPID [5], give equations that can be used to estimate slosh height h_s respectively. Moreover, as shown in Eq. (3), the predicted theoretical slosh height in the SPID [5] is suggested to be increased by 20% to account for higher sloshing modes of sloshing and nonlinear sloshing effects on upward sloshing movement observed during stronger shaking:

$$h_s = 0.6L \frac{S_a}{g} \quad (4)$$

where S_a is 0.5% damped horizontal design spectral acceleration of the ground or floor on which the tank is mounted at the frequency of the sloshing mode. For interior large-scale reinforced-concrete (RC) tanks in pressurized water reactor nuclear power plants (NPPs), such as spent fuel pools (SFP), the earthquake excitation is transferred by connecting floors which on the top and base of SFPs. SFPs are uncovered rectangular pools and are located in Fuel Buildings and usually near the elevations of ground. Fig. 1a depicts a typical configuration of SFP in a pressurized water reactor NPP [7]. The length, width and height of SFPs are about 50 feet, 30 feet and 40 feet, and a wall thickness of 5 feet approximately. The SFP contains about 40-feet depth water, and hence the frequency of sloshing mode (f_c) is estimated in the range of 0.2 to 0.4 Hz. On the other hand, the impulsive frequencies of SFPs are usually between 10 to 20 Hz and are higher than the



frequency content of general near-fault ground motions. Considering the fundamental frequencies of plant buildings in horizontal directions are mainly above 5 Hz and the locations of SFPs are at or near ground levels, the seismic response of the top portion of the fluid content in such tank is mainly controlled by the sloshing mode in low frequency, which might be resonant with low-frequency content of ground motion. As depicted in Fig. 1b, under the condition of the same zero period acceleration (0.67g), the 5% damped spectral acceleration values at the sloshing frequency of the near-fault ground motions recorded in 1999 Chi-Chi earthquake are higher than the value of the NUREG/CR-0098 design spectrum [8]. Based on Baker's study [9], general period of velocity pulse of near-fault ground motions is between 0.078 to 2.5 Hz. It implies that the sloshing mode is possibly resonant with near-fault ground motion and the slosh height of storage water would be much higher than the designed value, and hence loss of water might exceed the expected quantity.

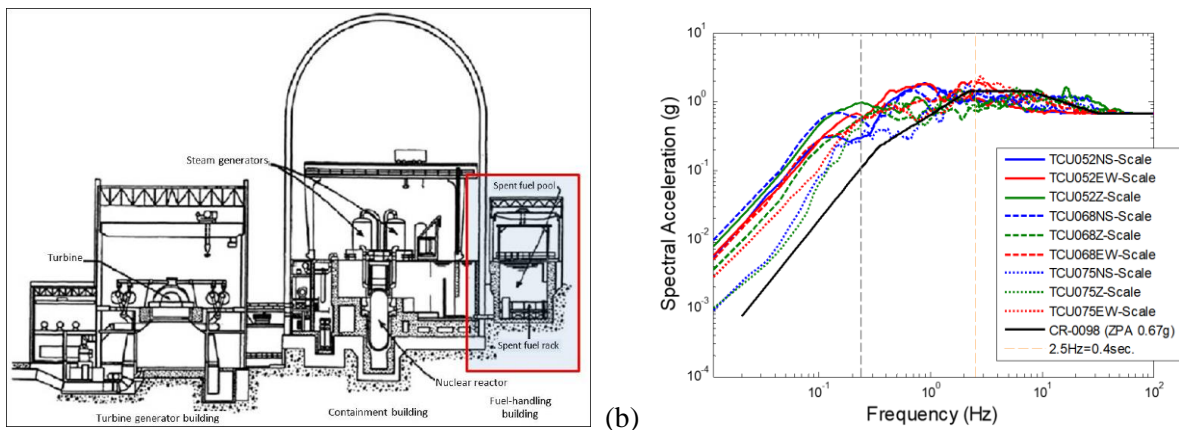


Fig. 1 – (a) A typical spent fuel pool in a power plant [7]; (b) Response spectrum of near-fault ground motion

This study aims to investigate the dynamic behavior of the sloshing mode and is focused to discuss the resonance phenomenon caused by the lower frequency content of near-fault ground motion on the contained water in relatively stiff rectangular tanks. In order to examine the rationality of the evaluation equations provided by guidelines, a series of shaking table tests were executed to discuss possible parameters which might influence the sloshing frequency (f_c) and slosh height (h_s). In this paper, the test plan including the design of tank specimen and input motion is described in detail. The preliminary analysis results are revealed to compare with the code-specified values.

2. Design of Tank Specimens

To investigate the sloshing behaviors of the stored water in the rectangular tanks, the shaking table tests for the rectangular and square scaled tanks were implemented. To design tank specimens, the sloshing frequencies of stored water in a rectangular or square tank need to be discussed. As dash lines in Fig. 2, the equation (1) and (2) give the relationship between the sloshing frequencies and depth of stored water-to-length ratio (H_L/L). The figure shows that the sloshing frequency will become higher and converge to a constant value as H_L/L increasing. Therefore, if a fixed dimension tank would like to be designed with lower sloshing frequency, the depth of stored water needs to be kept in a lower level. However, it needs to be considered that the lower water level might cause the bottom of the tank uncovered as water sloshing, which is a quite abnormal phenomenon for large-scale storage tanks even under strong earthquakes.

In the study, the scaled tanks were designed due to limitation of the dimensions of the shaking table, and the water levels were kept above specific level to avoid uncovered bottom of the tanks, and hence the sloshing frequencies were higher than usual sloshing frequencies of SFPs. To investigate the sloshing behaviors of different dimension of tanks, rectangular tank set was designed with inside width of 0.5 m and length of 1.0 m, and square tank set with inside length of 1.0 m respectively. The square tank set and the length of rectangular tank set were for $H_L/L = 0.5$, and the width of rectangular tank set was for $H_L/L = 1.0$. Both the



square and rectangular tank sets with equal water level were subjected to the same input motion simultaneously. By comparing the slosh height measured in square and rectangular tank sets, the effect of adjacent orthogonal side length can be clearly compared. On the other hand, there were two testing tanks with different height prepared for each tank set. The two tanks with equal water level were subjected to the same input motion simultaneously, such that the slosh height could be measured from the higher tank, and the volume of water splashing out of tank could be estimated from the lower tank. Therefore, the relationship between the slosh height, freeboard and the associated total volume of water splashing out of tank could be found. Based on considerations mentioned above, the sloshing frequencies along the length and width of rectangular tanks were designed below 1.25 Hz per equation (1) as shown in Fig. 2. In the design, the tanks were considered as rigid tanks. It means that the fundamental frequency of the tank is much higher than the sloshing frequencies of the stored water. Finally, the tanks were made of A36 steel. As shown in Fig. 3a, outside each scaled tank is a water receiving tank to prevent water splashing to the shaking table. In order to avoid sliding behavior of specimens occurred during tests, the tank specimens are anchored with more than 20 M30 bolts for each to the shaking table (Fig. 3b).

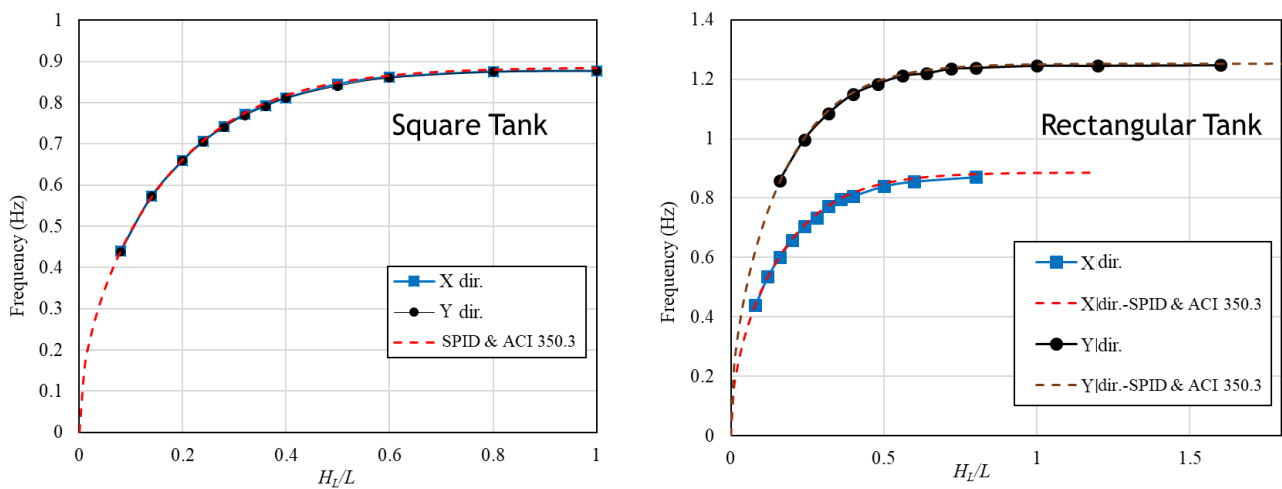


Fig. 2 – The relationship between sloshing frequencies and H_L/L of stored waters in tanks

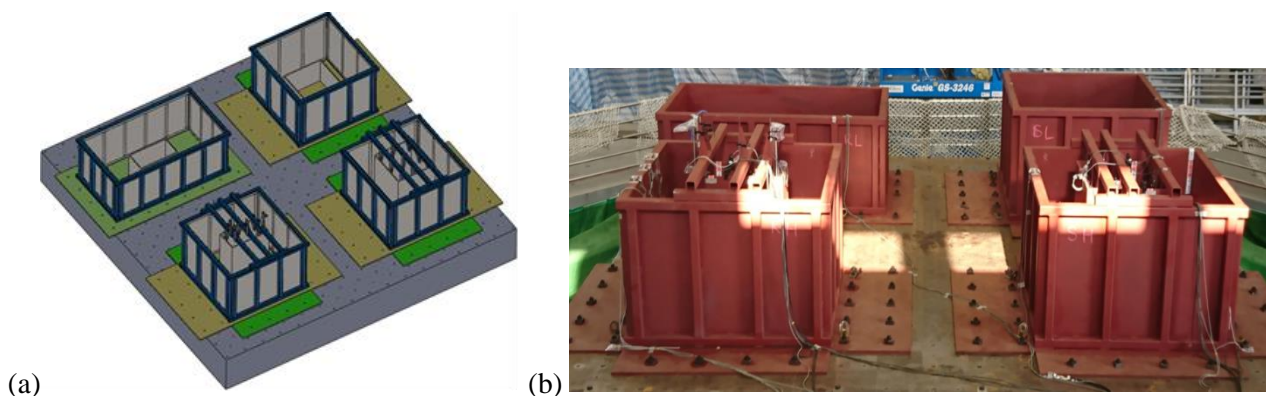


Fig. 3 – Specimens of scaled tanks: (a) numerical models; (b) test configuration



3. Input Motion of Shaking Table Tests

In order to focus on possible unpredicted effects on sloshing behavior of stored waters in rectangular tanks caused by near fault ground motions, a series of shaking table tests were executed on the 6 DOF 8m x 8m shaking table in NCREE Tainan Laboratory. The shaking table is designed to perform near-fault ground motions with the frequency contents in the range from 0.1 to 30 Hz. In this study, the largest scale of input motions are limited by the capacity of stroke or velocity of the shaking table (Table 1). In order to investigate basic dynamic characteristics and seismic behavior of contained water, test types and respective input motions are designed as below (Fig. 4):

Table 1 – Performance of the shaking table

Axis	X axis	Y axis	Z axis
Stroke	±1.0 m	±1.0 m	±0.4 m
Velocity	±2.0 m/sec	±2.0 m/s	±1.0 m/s
Acceleration			
250t specimen	±0.75 g	±0.75 g	±0.5 g
100t specimen	±1.4 g	±1.4 g	±0.8 g
Bare Table	±2.5 g	±2.5 g	±3.0 g
Overturning Moment Limit: 500 ton-m (biaxial), 1000 ton-m (uni-axial)			

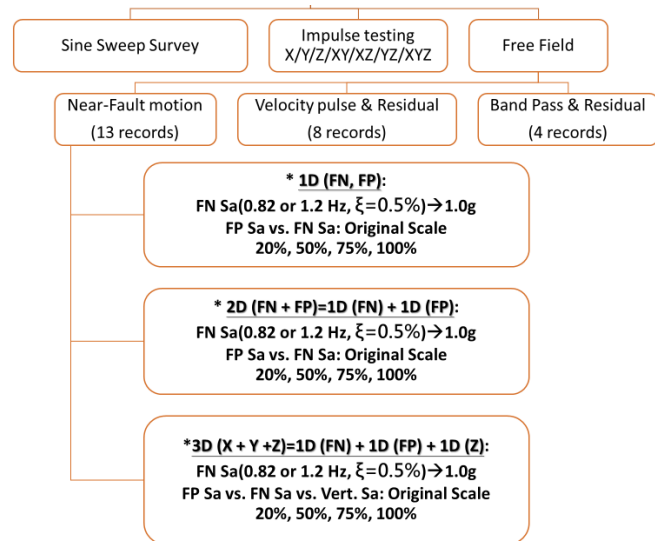


Fig. 4 – Categories of input motions

- (1) System-identification tests: Sine-sweep survey and impulse tests were adopted in this study. The purpose of the sine-sweep survey is to obtain more distinct modal shape of water surface. On the other hand, natural frequencies and damping of the sloshing mode of the contained water can be obtained during the free vibration after impulse to exclude the disturbance of excitation. Both kinds of input motion are designed to excite equal response of each tested contained water with the sloshing frequency in the range from 0.3 Hz to 2 Hz. The spectral acceleration values of the impulse motion in the range from 0.3 to 2 Hz are about 0.14g. According to the dimension of four tank specimens depicted above, the sloshing frequencies of varied water levels and slosh height are predicted based on the spectral acceleration of both types of inputs to exclude the possibility of splashing out during system-identification tests.

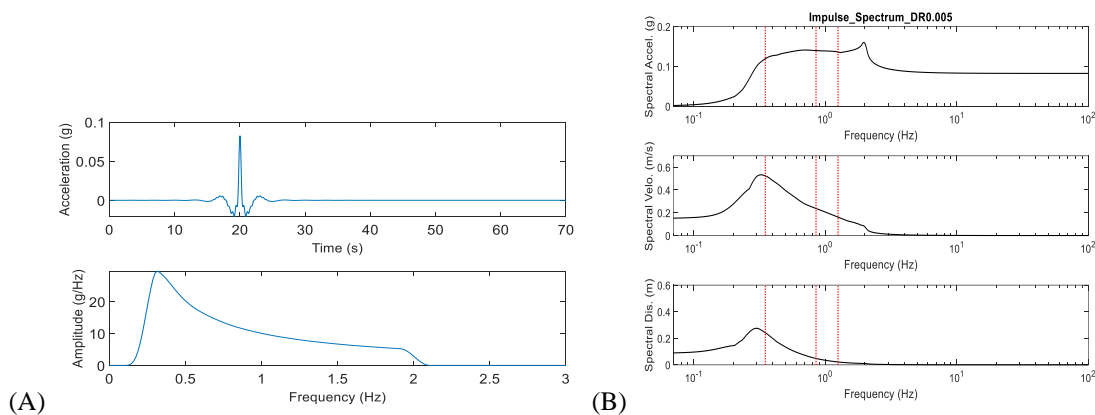


Fig. 5 – Impulse motion for system identification: (a) time history and Fourier spectrum; (b) response spectra



(2) Near-fault ground motion tests: Referring to the definition proposed by Baker [9], 91 near-fault motions with pulse-like property are picked out first from 3551 records stored in the PEER NGA West database [10]. The database provides period of velocity pulse (T_P) through wavelet analysis and the period of peak spectral velocity (T_{Sv}) of the Fault-normal (FN) component of each ground motion as well. Based on the designed water level (0.5m) and tank dimensions, the sloshing frequencies can be predicted as 0.84 Hz and 1.2 Hz for the direction with length of 1.0 m and 0.5 m respectively. As shown in Table 2, Fig. 6 and Fig. 7, in order to observe possible effects caused by resonant response or long-period velocity pulse on slosh height, 13 records of 7 earthquake events are picked out from 91 records based on the comparison of T_P and T_{Sv} values. The selection criteria are described as below:

- a. Type A--Both T_P and T_{Sv} are much smaller than 0.8 seconds (higher than 1.2 Hz): Record Sequence Number (RSN) 1050 is selected to observe potential high-mode effects on slosh height due to the small T_P and T_{Sv} values and relatively large spectral response in the high-frequency range;
- b. Type B--Both T_P and T_{Sv} are about 0.8 seconds (1.2 Hz) or 1.2 seconds (0.84 Hz): This type is expected to excite unexpected resonant response of water, which is not considered per equation (1). For sloshing frequency of 1.2 Hz, the corresponding input motions include the FN components of RSN 1051, RSN 568 and RSN 451, and the FP component of RSN 1550. For sloshing frequency of 0.84 Hz, the corresponding input motions include RSN 1063, RSN 459 and RSN 1120 in FN direction, and RSN 459 in FP direction;
- c. Type C-- T_P is much larger but T_{Sv} is about 0.8 seconds (1.2 Hz) or 1.2 seconds (0.84 Hz): In order to distinguish effects of T_P and T_{Sv} , the values of T_{Sv} of FN components of RSN 1119 and RSN 900 are near the sloshing frequency of 1.2 Hz, while those of T_{Sv} of FN components of RSN 828 and 1550 are near the sloshing frequency of 0.8 Hz;
- d. Type D--Both T_P and T_{Sv} are much larger than 0.8 seconds (smaller than 1.2 Hz) or 1.2 seconds (0.84 Hz): At the same spectral acceleration value, this kind of ground motions, RSN 1529 and RSN 1481, is to dig out possible effects of other parameters.

According to the equation (3) and (4), the slosh height h_s is controlled by the spectral acceleration at sloshing frequency. In order to observe other parameters of near-fault ground motion with possible influence on slosh height, the FN component of tested ground motion and the FP component of RSN 1050 are scaled to anchor the 0.5% damped spectral acceleration to 1.0g at the sloshing frequency of 0.84Hz or 1.2 Hz. The scaled FN, FP and vertical components of each ground motion are kept in the original proportion unless restricted by the shaking table limits (Table 1).

Table 2 – Basic information of ground motions

RSN	Event	Station	T_P (sec)		T_{Sv} (sec)	
			FN	FP	FN	FP
1050	Northridge-01	Pacoima Dam (downstr)	0.481	1.094	0.455	0.909
568	San Salvador	Geotech Investig Center	0.850	1.799	0.667	0.769
1051	Northridge-01	Pacoima Dam (upper left)	0.891	0.454	0.667	0.303
451	Morgan Hill	Coyote Lake Dam (SW Abut)	0.946	1.053	0.769	0.769
1063	Northridge-01	Rinaldi Receiving Sta	1.214	3.041	1.429	0.370
459	Morgan Hill	Gilroy Array #6	1.225	1.053	1.111	0.833
1120	Kobe, Japan	Takatori	1.627	2.964	1.111	1.250
1119	Kobe, Japan	Takarazuka	1.433	1.753	1.250	0.476
828	Cape Mendocino	Petrolia	2.592	0.957	0.625	0.769
900	Landers	Yermo Fire Station	7.637	2.685	1.429	2.500
1481	Chi-Chi, Taiwan	TCU038	8.436	8.375	5.000	0.385
1529	Chi-Chi, Taiwan	TCU102	9.387	3.467	2.500	2.500
1550	Chi-Chi, Taiwan	TCU136	10.918	7.003	0.909	1.000

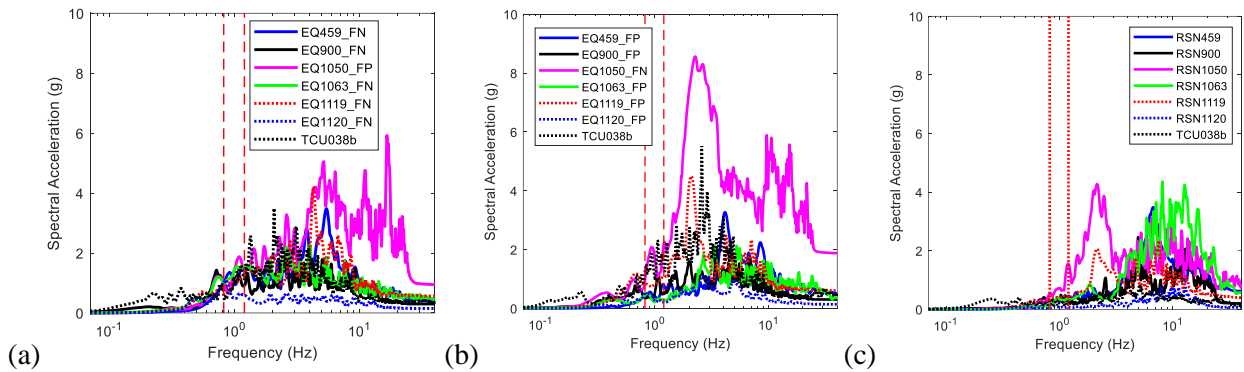


Fig. 6 –Normalized near-fault ground motions for square tanks in: (a) X, (b) Y and (c) Z directions.

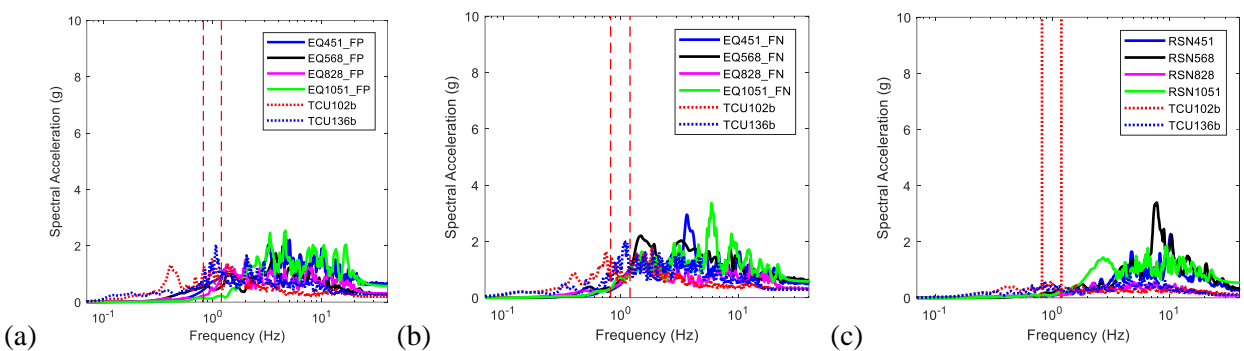


Fig. 7 – Normalized near-fault ground motions for rectangular tanks in: (a) X, (b) Y and (c) Z directions.

- (3) Velocity-pulse (VP) and residual motion (RVP) tests: In order to clarify the effects of velocity pulse at resonant or non-resonant frequency on slosh height with the comparison to the original near-fault ground motion test results, the velocity pulses and residual ones are extracted from RSN 451, RSN 459, RSN 900, RSN 1550 and RSN 1063 with the Matlab codes of wavelet analysis provided by Baker [8]. Comparing to other motions of Type B, RSN 451 resulted in more significant resonant sloshing phenomenon since the T_p values of FN and FP components are 0.946 sec and 1.053 sec respectively, which are both close to 0.8 sec. In order to further study the influence of long-period energy on sloshing behavior, RSN 900 and 1550 are selected due to its remarkable characteristics of long-period pulse in three components. Take RSN 900 as an example (Fig. 8), the FN and FP velocity pulses (depicted as red lines) of RSN 900 are extracted with T_p values of 7.637 sec and 2.685 sec respectively. Meanwhile, the residual motions (depicted as back lines) keep other frequency content including sloshing frequency of 0.8Hz to 1.2 Hz and T_{sv} of 0.7 Hz. By the comparison among the slosh height values resulted from the original near-fault ground motion, velocity-pulse or residual ones, the contribution from long-period pulse energy or resonant response to the sloshing behavior can be clarified.

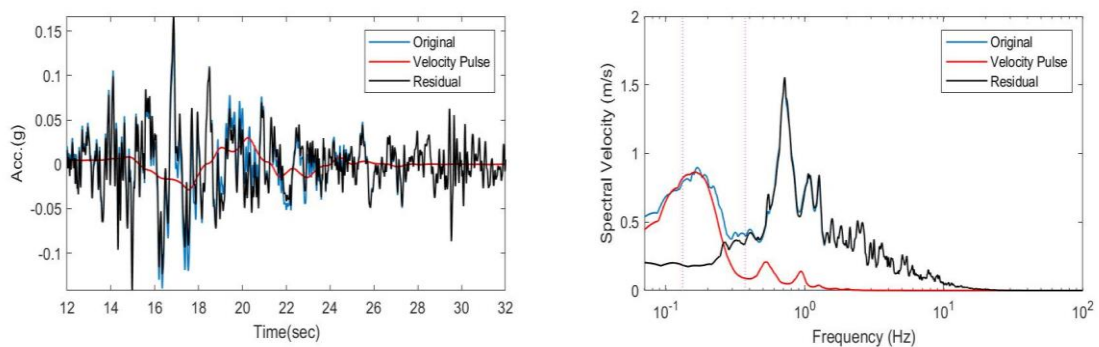


Fig. 8 – Acceleration time histories and velocity response spectra of RSN 900 in FN direction.



- (4) Band-pass and residual motion tests: In addition to the wavelet analysis of velocity time histories, band-pass frequency analysis for acceleration of RSN 900 and 1550 are also derived in the frequency range of 0.730 Hz to 1.324Hz. As shown Fig. 9, the blue lines represent band-pass motion and corresponding response spectra. According to the Equation (3) and (4), since the spectral acceleration values of band-pass motion are almost the same as original ground motions (black lines), the band-pass motion is predicted to excite resonant response of water sloshing as original ground one.

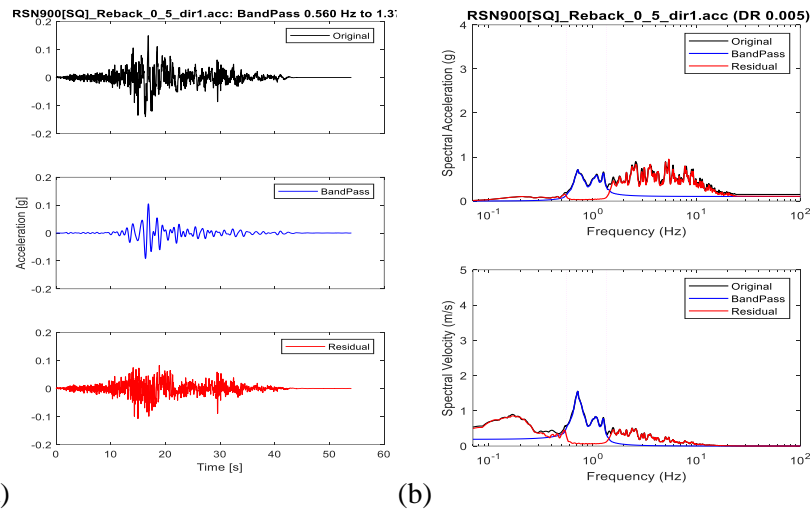


Fig. 9 – (a) Acceleration time histories and (b) response spectra of RSN 900 in FN direction.

4. Test Configuration

During shaking-table tests, accelerometers and magnetostrictive linear-position sensors (Temposonic transducers) were used to record responses of tank specimens and water contents. As shown in Fig. 10a, four $\pm 5g$ tri-axial accelerometers were arranged at the steel bottom plate and the top of the square and rectangular tank walls respectively to record acceleration response of tank specimens. The recorded acceleration data are used to examine that the tanks are rigid enough to minimize the influence of impulsive modes on the dynamic response of water. 19 displacement transducers are used for water level sensing applications. As shown in Fig. 10a and Fig. 10b, 4 action cameras for each tank were attached directly on the top of the tank walls to record the whole test process of the movement of water surface of water. The video records were also used to observe the sloshing and waving condition of water surface and ensure the accuracy of water level measurements of transducers by watching the achieved water levels noted by attached waterproofing rulers.

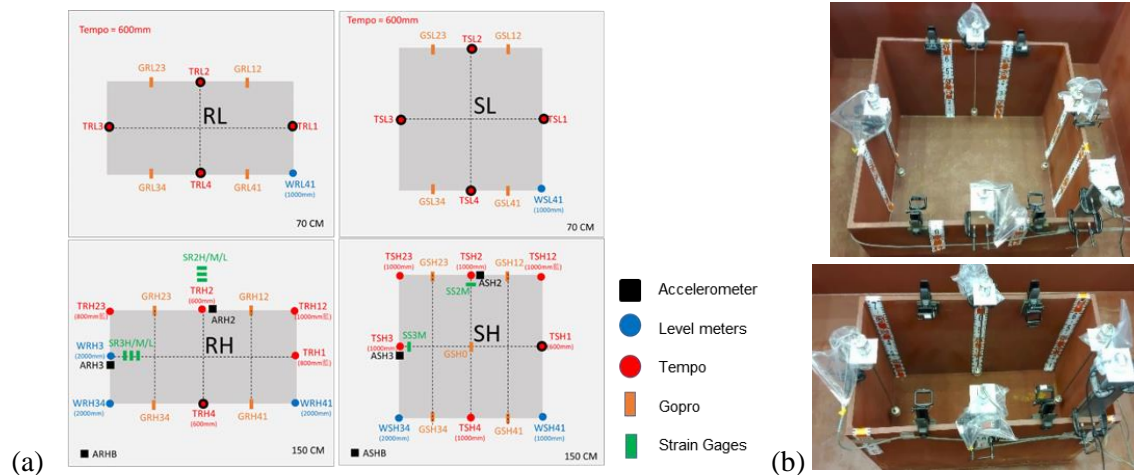


Fig. 10 – Instrument configuration



During system-identification tests, different water levels were selected to verify the accuracy of evaluation equation (1) for sloshing frequency. A series of water levels from 8cm to 100cm are adopted to envelope the range of gradual change and convergence of the relationship between sloshing frequency and water level (Fig. 2). For each tested water level, uniaxial, biaxial and triaxial tests are arranged to observe the effects of multi-axis inputs and the direction of vertical motion on sloshing frequency and damping of water.

On the other hand, a total of 180 seismic tests were executed in this study. Table 3 depicts the test procedure of seven ground motions selected from PEER NGA West database. Table 3 also shows that because several ground motions cannot be 100% executed and limited by maximum displacement capacity of shaking table, therefore, the maximum scale for each motion is decrease to 75%. As described in the above section, the spectral acceleration at 0.84Hz or 1.2 Hz of the FN component of each ground motion is normalized to 1.0 g, and scaled down to 20%, 50% and 75% respectively to observe possible nonlinear increase of slosh height. In addition, 50% velocity pulse (VP), residual velocity pulse (RVP), band pulse (BP) and residual band pulse (RBP) tests of RSN451, 459, 900, 1063 and 1550 were executed in this study. Uniaxial (X, Y or Z), biaxial (X and Y) and tri-axial tests are arranged to compare the slosh height under multi-axis inputs to the one evaluated by SPID [5] or Chen [6].

Table 3 Procedure of system identification tests

Ground Motion	Input direction	Intensity	Ground Motion	Input direction	Intensity
RSN1050	X/Y/XY/XYZ	20%/50%/75%	RSN451_VP	X/Y/XY/XYZ	50%
RSN568	X/Y/XY/XYZ	20%/50%/75%	RSN451_RVP	X/Y/XY/XYZ	50%
RSN1051	X/Y/XY/XYZ	20%/50%/75%	RSN459_VP	X/Y/XY/XYZ	50%
RSN451	X/Y/XY/XYZ	20%/50%/75%	RSN459_RVP	X/Y/XY/XYZ	50%
RSN1063	X/Y/XY/XYZ	20%/50%/75%	RSN900_VP	X/Y/XY/XYZ	50%
RSN459	X/Y/XY/XYZ	20%/50%/75%	RSN900_RVP	X/Y/XY/XYZ	50%
RSN1120	X/Y/XY/XYZ	20%/50%/75%	RSN900_BP	X/Y/XY/XYZ	50%
RSN1119	X/Y/XY/XYZ	20%/50%/75%	RSN900_RBP	X/Y/XY/XYZ	50%
RSN828	X/Y/XY/XYZ	20%/50%/75%	RSN1550_VP	X/Y/XY/XYZ	50%
RSN900	X/Y/XY/XYZ	20%/35%/50%/75%	RSN1550_RVP	X/Y/XY/XYZ	50%
RSN1481	X/Y/XY/XYZ	20%/35%/50%	RSN1550_BP	X/Y/XY/XYZ	50%
RSN1529	X/Y/XY/XYZ	20%/50%/75%	RSN1550_RBP	X/Y/XY/XYZ	50%
RSN1550	X/Y/XY/XYZ	20%/50%	RSN1063_VP	X/Y/XY/XYZ	50%
			RSN1063_RVP	X/Y/XY/XYZ	50%

5. Preliminary Test Results

5.1 Frequency

From the measured data of acceleration at the tank specimens, the tank frequencies are above 30 Hz and are much higher than the frequency content of input motions and the sloshing frequencies of contained water. It implies that the effect of the impulsive mode might be neglected in the analysis of dynamic behavior of sloshing modes. On the other hand, Fig. 2 shows the relationship of measured sloshing frequency and H_l/L . Dash lines is the theoretical sloshing frequencies of each water level evaluated per equations (3) and (4). The blue and black lines depict the relationship between experimental sloshing frequency and H_l/L ratio under horizontal impulse motions. From Fig. 2, it can be seen that experimental sloshing frequencies are quite close to but



slightly higher than the theoretical values. Furthermore, in this study, it is confirmed that the effect of vertical input on the sloshing frequency is not so significant.

5.2 Damping

According to the ACI 350.3-06 [4], the convective response damping ratio for water content is 0.5%. In order to verify the validity of the designated value of damping ratio, the results of impulse tests are analyzed using the measurement values of Tempsonic sensors. Assuming the sloshing behavior of water content in tank specimens performs as a single degree of freedom, both logarithmic decrement method and half-power method are adopted to calculate sloshing frequency based on the free oscillating response during the impulse test. Taking the negative amplitude measured by the SH1, SH2, SL1, SL2, RH1, RH2, RL1 and RL 2 sensors, the damping ratio is calculated along the length or width of square or rectangular tanks. Taking damping ratios along the 1.0m-direction of tanks for an example, the relationship between the damping ratio and water level under uniaxial or biaxial tests are expressed in the Fig. 11. It can be seen that the influence of the direction of impulse input on the damping ratio is quite small. However, the damping ratio decreased dramatically while the water-to-length ratio (H/L) decreases from 0.08 to 0.2, and is converged to about 0.35%, which is slightly smaller than the value of 0.5% specified in ACI 350.3-06 [4] or SPID [5]. Considering depth of stored water-to-length ratio (H/L) was designed to be 0.5 or 1.0 under ground motion tests, damping ratio of 0.35% is conservatively adopted to apply Eq. (3) and Eq. (4) per Chen[6] and SPID [5] to evaluate slosh height.

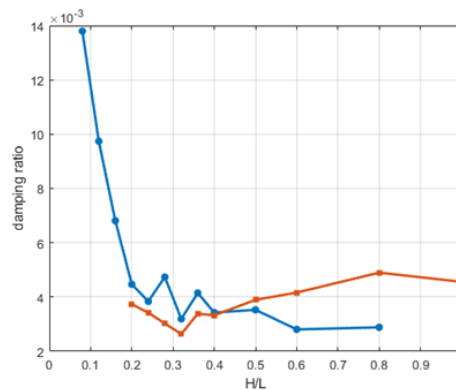


Fig. 11 – Damping ratio along X axis of the shaking table

5.3 Slosh height

Fig. 12 depicts the test results under uniaxial excitation. The abscissa of each point represents input spectral acceleration at the convective frequency according to the test conditions ($H_L=0.5\text{m}$ and $L=0.5\text{ m}$ or 1.0m), while the ordinate being the ratio of measured slosh height to the value evaluated by SPID [5]. Spectral acceleration is calculated with damping ratio of 0.35%. In addition, the measured slosh heights and the ones evaluated by SPID [5] and Chen[6] can be also compared in Fig. 13. It can be seen from Fig. 12 and Fig. 13 that evaluated results per SPID [5] is conservative for most test cases. However, it is still evident that in some cases the slosh height recorded from experiment extremely exceeds theoretical one. According to test results, other influence factors might be further considered under strong input motion.

In reality, the input motions with two orthogonal horizontal components should be considered for the rectangular tanks like SFP under earthquakes. In SPID [5], the total slosh height is estimated by:

$$h_{st} = \sqrt{h_{sx}^2 + h_{sy}^2} \quad (5)$$

where h_{sx} and h_{sy} represent slosh height in x- and y- direction respectively. The bi-axial excitation were tested in this study, and Fig. 14a depicts the relationship between the slosh height measured at corners of tank and the SRSS (square root of the sum of the squares) of slosh height measured at the midpoints of side walls in



both x- and y- directions. On the other hand, Fig. 14b depicts the relationship between the measured maximum slosh height and the SRSS of slosh heights in both x- and y- directions evaluated by equation (4) for 1D excitation. It shows that the maximum slosh height under bi-axial excitation can be evaluated well by equation (5) using h_{sx} and h_{sy} determined by equation (4) for 1D excitation, but not determined from the measured slosh height in x- and y- directions. It is because the slosh height measured at the side walls under 2D excitation is less than the value predicted by equation (4) for 1D excitation due to the two-dimensional interaction effect.

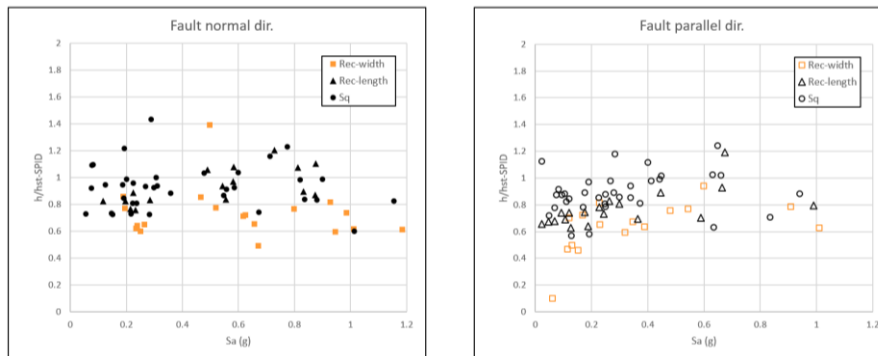


Fig. 12 –Ratio of slosh height and evaluated height per SPID [5] in FN (left) and FP (right) directions

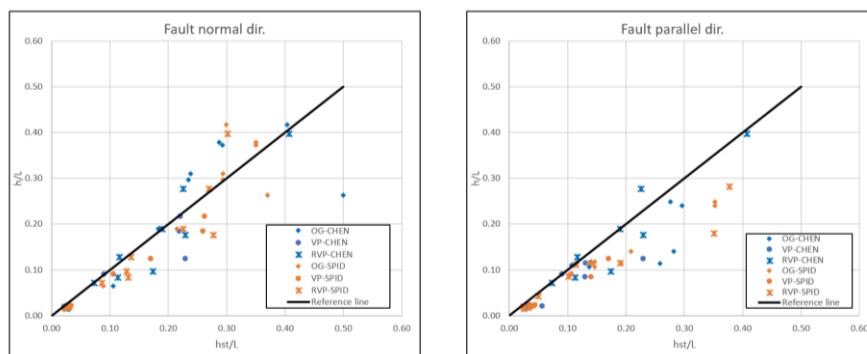


Fig. 13 – Relationship between ratio of measured slosh height to side length (h/L) and ratio of evaluated value to side length ($h_{s/L}$) per SPID [5] or Chen [6] in FN (left) and FP (right) directions

6. Summary

The purpose of this experiment is to estimate the slosh height and the associated total volume of water splashing out of the tank under near-fault ground motions. Seven near-fault ground motions are picked out to discuss effects of resonant response and velocity pulse, and a total of 180 seismic tests were executed. On the other hand, the validity of evaluation method for the frequency and slosh height and designated damping ratio value of sloshing mode provide by SPID [5] and ACI350.3-06 [4] are discussed based on the results of system identification tests. From preliminary test results and previous study for circular tanks [11], it can be seen that the evaluation of convective frequency is quite accurate under free vibration. However, the observed damping ratio decreased dramatically while the depth of stored water-to-length ratio (H_1/L) higher than 20 cm. The value of damping ratio is converged to about 0.35%, which is smaller than the value of 0.5% specified in ACI350.3-06 [4]. On the other hand, although SPID [5] is conservative for most of the test case, slosh height under two-dimension input motion might exceeds predicted values per SPID [5]. Thus, the evaluation method for slosh height is recommended to consider other possible influence factors, and it will be discussed in the future study.

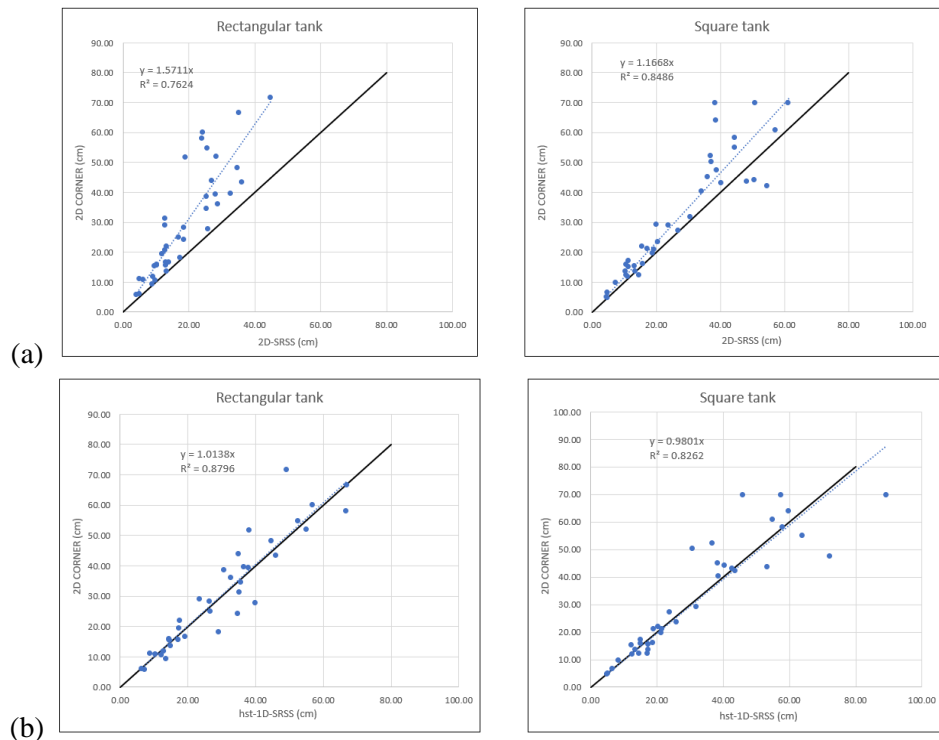


Fig. 14 –Relationship between maximum slosh height under 2D excitation and (a) SRSS of slosh height measured at side walls, and (b) SRSS of slosh heights evaluated for 1D excitation

7. References

- [1] The Seismic Qualification Utility Group (SQUG), *Seismic evaluation training course*, Rev. 4.2, 2008.
- [2] Tokyo Electric Power Company (TEPCO), *Impact of the Niigata Chuetsu-oki Earthquake on the TEPCO Kashiwazaki-Kariwa Nuclear Power Station and Countermeasures*, 2007.
- [3] Haroun, M.A. & Housner, G.W. *Seismic design of liquid-storage tanks*, Journal of the Technical Councils of the American Society of Civil Engineers, Vol. 107, No. TCI, pp. 191-207, 1981
- [4] ACI Committee 350.3-06, *Seismic Design of Liquid-Containing Concrete Structures and Commentary*, American Concrete Institute, Farmington Hills, MI, 2010.
- [5] EPRI, *Seismic Evaluation Guidance- Screening, Prioritization, and Implementation Details (SPID) for the Resolution of Fukushima Near-Term Task Force Recommendation 2.1: Seismic*, EPRI Report 1025287, 2013.
- [6] W. Chen, M. A. Haroun & F. Liu, Large amplitude liquid sloshing in seismically excited tanks, *Earthquake Engineering and Structural Dynamics*, Vol.25, Issue7, pp. 653-669, July 1996.
- [7] EPRI (2017), “Seismic Evaluation Guidance: Spent Fuel Pool Integrity Evaluation,” EPRI Report 3002009564.
- [8] Newmark N. M. & Hall W. J., *Development of Criteria for Seismic Review of Selected Nuclear Power Plants*, Technical Report NUREG/CR-0098, U.S. NRC, May 1978.
- [9] Jack W. Baker, *Quantitative Classification of Near-Fault Ground Motions*, Bulletin of the Seismological Society of America, Vol. 97, No. 5, pp. 1486–1501, October 2007.
- [10] PEER Center, University of California, PEER NGA West database, <https://ngawest2.berkeley.edu/>
- [11] J.-F. Chai , F.-R. Lin, W.-H. Hsu, T.-C. Chien, Z.-Y. Lai, Z.-Y. Lin, *experimental study of near-fault effect on sloshing mode of storage liquid in tanks*, PVP2019- 93388, Proceedings of the ASME 2019, San Antonio, TX, USA.